Comunicações Geológicas

Comunicações Geológicas (2025) 112, 1, 79-87

ISSN: 0873-948X; **e-ISSN:** 1647-581X

Identification of saline areas in wetlands using spectral indices and geochemical data. The case of Baixo Vouga Lagunar (Aveiro, Portugal)

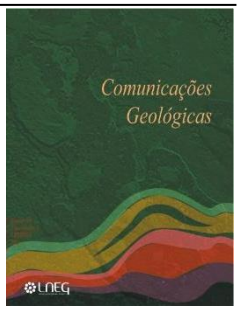

Identificação de áreas salinas em zonas húmidas com recurso a índices espetrais e dados geoquímicos. O caso do Baixo Vouga Lagunar (Aveiro, Portugal)

R. S. V. Rolo[1], S. M. L. Silva[2], J. Medina[1,3*], C. Patinha[1,3]

DOI: https://doi.org/10.34637/r0fp-z138

Recebido em 19/04/2025 / Aceite em 12/12/2025

Publicado online em janeiro de 2026

Original article
Artigo original

Abstract: The Baixo Vouga Lagoon (BVL) is an important wetland on the Portuguese coastal continent that has been suffering from the destruction of its agricultural fields due to saline intrusion processes. The aim of the research was to identify areas of salinity combining geochemical data and spectral indices obtained from Sentinel 2B satellite images. The methodology was developed using images from July 2023 and February 2024, with samples taken during the same seasonal period. Fourteen spectral indices were calculated: four vegetation indices and ten salinity indices. Pearson's method was used to assess the correlation between geochemical data and the spectral indices. The Canopy Response Salinity Index (CRSI) and Salinity Index 1 (SI 1) showed the highest correlation, at 0.428 and 0.516 respectively. Despite the limitations of using optical sensor in flooded areas, the spectral response of halophyte vegetation in areas of higher salinity was crucial for its differentiation and primary delimitation of the most affected areas.

Keywords: Remote sensing, Baixo Vouga Lagunar (BVL), Sentinel-2, salinity, Halophytes.

Resumo: A região do Baixo Vouga Lagunar (BVL) é uma importante zona húmida do continente costeiro português que tem sofrido com o problema da destruição dos seus campos agrícolas, devido a processos de intrusão salina. O objetivo de pesquisa foi identificar áreas de salinidade através da combinação de dados geoquímicos e índices espetrais obtidos através de imagens do sistema de satélite *Sentinel 2B*. A metodologia foi desenvolvida utilizando imagens referentes aos meses de julho de 2023 e fevereiro de 2024, estando as amostras situadas no mesmo período sazonal. Foram calculados catorze índices espetrais a partir das imagens de satélite: quatro índices de vegetação e dez índices de salinidade. O método de *Pearson* foi usado para avaliar a correlação entre os dados geoquímicos e os índices espetrais. O Índice de Resposta do Dossel à Salinidade (CRSI) e o índice de salinidade SI 1 foram os que apresentaram maior correlação, na ordem de 0,428 e 0,516, respetivamente. Apesar das limitações do uso de sensores óticos em áreas inundadas, a resposta espectral da vegetação halófita, presente nas áreas de maior salinidade, foi crucial para a sua diferenciação e delimitação primária das zonas mais afetadas.

Palavras-chave: Deteção remota, Baixo Vouga Lagunar (BVL), Sentinel-2, salinidade, Halófitas.

[1] Department of Geosciences, University of Aveiro, 3810-193 Aveiro, Portugal.

[2] Cartography Department, Engineering Faculty, State University of Rio de Janeiro (UERJ), Rio de Janeiro, Brazil.

[3] GeoBioSciences, GeoTechnologies and GeoEngineering (GEOBIOTEC), Department of Geosciences, University of Aveiro, 3810-193 Aveiro, Portugal.

* Corresponding author / Autor correspondente: jmedina@ua.pt

1. Introduction

The increasing salinization of soils around the world has been one of the main conditioning factors for agricultural crops, affecting their quality and productivity. This growing salinization is linked to population expansion and climate change, implying an increase in the need for fresh water and agricultural production leading to erroneous irrigation techniques. Climate change causes a decrease in the rate of precipitation and an increase in evapotranspiration in arid and semi-arid zones, which leads to the formation of salts on the soil surface (Vengosh, 2014).

The accumulation of salt in the soil profile causes degradation and a reduction in the photosynthetic activity of plants, caused by disruption of the DNA and proteins, preventing the uptake of nutrients and water (Bratovcic, 2024). However, there are groups that are more resistant to salinity, such as halophytic plants. Salinity is studied by taking samples, which can be a time-consuming and expensive process. Remote sensing is a simplified method for assessing and identifying salinity in large areas.

The Baixo Vouga Lagunar (BVL) is an important wetland on the Portuguese mainland coast, influenced by tidal action and frequent flooding, and is a barrier protecting the coast and a habitat for important animal and plant species (Silva, 2000). This agro-ecosystem is highly vulnerable and is the target of progressive degradation due to saline intrusion, which damages the region's agricultural soils (Lopes and Andresen, 2009). The loss of these soils has a major economic and environmental impact, which makes it essential to develop studies to monitor the current state, distribution and evolution of salinity.

Since 1975, projects have been developed to create infrastructure to protect the BVL area, such as the "Execution Project of the Tidal Protection Dike", which included work to build a continuous stretch of three dikes: one to the south, one to the north and another in

between, already built and located between the Rio Velho and the mouth of the Rio Antuã. In addition to this, other infrastructures would be built to safeguard access to the region, prevent the progression of the tide and allow the flow of water during floods. However, in 2005, due to problems with approval, the project was scrapped, resulting in saltwater entering through the middle. The project was studied again in 2017, but the complete construction of the dike is under public tender until today.

It is important to mention that previous studies on soil salinity in regions with salt-adapted plants have predominantly focused on spectral indices based on hypersaline environments within areas with arid and semi-arid climates (Kurbatova *et al.*, 2021). The geochemical validation with the spectral behavior of soil and halophytic vegetation, contributes to a comprehensive understanding of salinization patterns in wetland environments, especially in temperate climates.

Based on the above, the main objective of this study is to map the salinity of soils in the BVL region by combining spectral indices, geochemical data and the spatial distribution of halophytic vegetation.

2. Materials and Methods

2.1. Area of Study

The BVL (Baixo Vouga Lagunar) is located in the district of Aveiro, in the central area of the Portuguese continental coast and covers three municipalities: Albergaria-a-Velha, Aveiro and Estarreja (Fig. 1). It occupies an area of about 4600 hectares and is a wetland with high agricultural, economic, natural and socio-cultural potential (Lopes and Andresen, 2009). It has an average annual temperature of around 15 ºC, reaching values above 30 ºC in the summer months and around 10 ºC in the winter months with average annual rainfall values around 800 mm, consequently classified as a temperate climate.

The study area is commonly divided into three landscaping units: Open Field, Wetlands and Bocage that vary according to the amount of water, land use and habitats involved (Fig. 1). In the Open fields, agricultural production is primarily dominated by

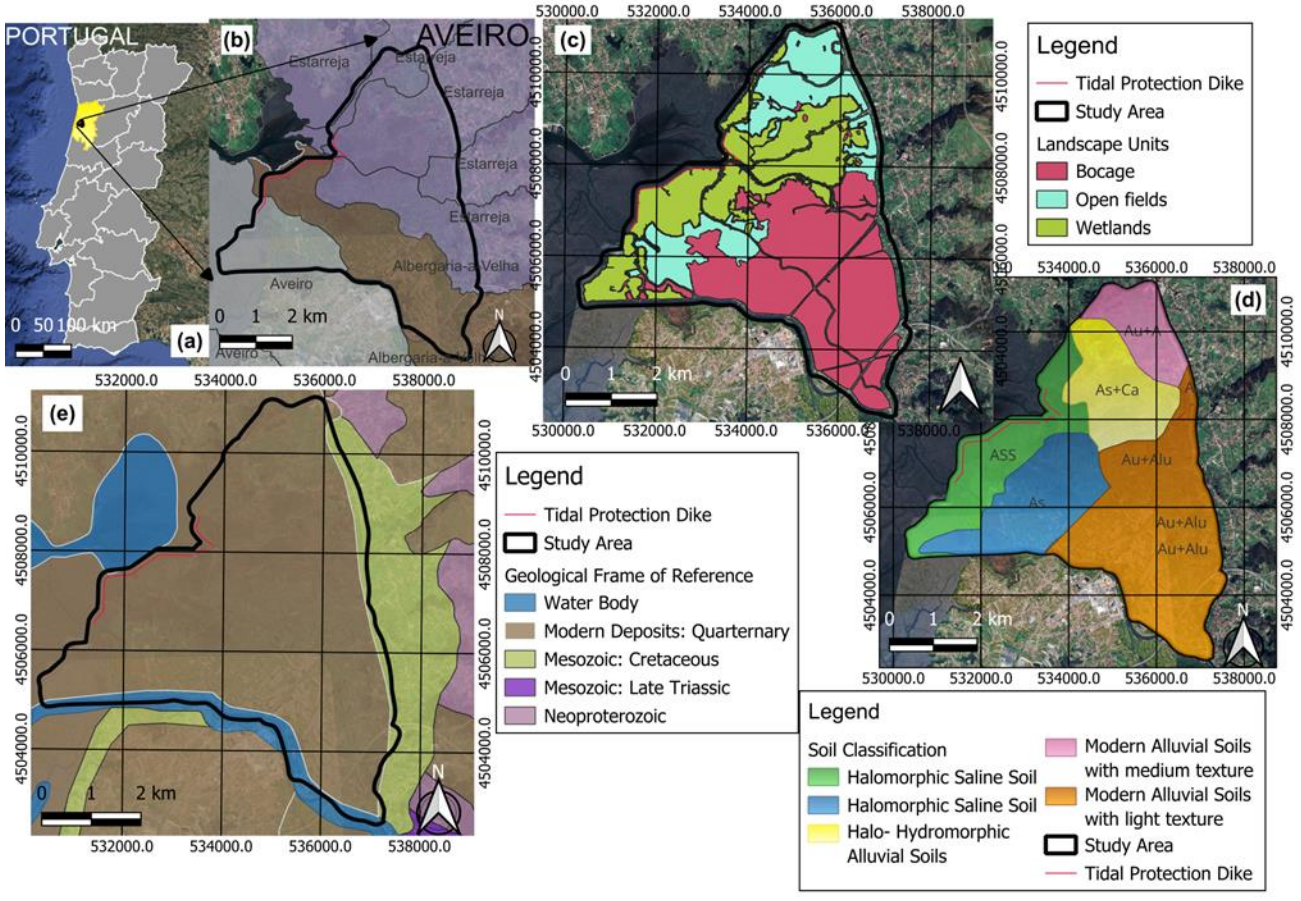

Figure 1. Spatial characterization of the Baixo Vouga Lagunar (BVL) according to the WGS 84 reference system and UTM 29N zone projection system. (a) Geographic location of Portugal with emphasis on the Aveiro district; (b) municipal boundaries comprising the BVL area (Estarreja, Albergaria-a-Velha and Aveiro); (c) landscape Units of BVL; (d) pedological classification of BVL; (e) geological framework of the BVL. Base shapefiles were obtained from Portuguese institutional databases, including sources such as DGT (Direção-Geral do Território), SNIG (Sistema Nacional de Informação Geográfica), and LNEG (Laboratório Nacional de Energia e Geologia).

Figura 1. Caracterização espacial do Baixo Vouga Lagunar (BVL) de acordo com o sistema de referência WGS 84 e o sistema de projeção de zona UTM 29N. (a) Localização geográfica de Portugal com destaque para o distrito de Aveiro; (b) limites municipais que compõem a área do BVL (Estarreja, Albergaria-a-Velha e Aveiro); (c) unidades paisagísticas do BVL; (d) classificação pedológica do BVL; (e) contexto geológico do BVL. Os ficheiros *shapefiles* de base foram obtidos a partir de bases de dados institucionais portuguesas, incluindo fontes como a DGT (Direção-Geral do Território), o SNIG (Sistema Nacional de Informação Geográfica) e o LNEG (Laboratório Nacional de Energia e Geologia).

corn and rice cultivation. The wetland systems comprise marshes and reed beds, which function as key ecological habitats and migratory corridors for various bird species. The Bocage represents a rare anthropogenic landscape in Portugal, characterized by a distinctive mosaic pattern that integrates agricultural fields, pastures, and transitional zones between them. The Baixo Vouga Lagunar is affected by the direct action of tidal dynamics, which allows a permanent flow of saline water into its landscaping units. Changes in the maintenance of coastal systems, geomorphology of the lagoon, and the flooding phenomena themselves have allowed the increase of saline intrusion, which constitutes a significant risk, particularly to agricultural activities in the region.

The soils within the study area consist primarily of halomorphic and hydromorphic alluvial soils (SROA, 1970; Cardoso, 1974). Associated with these are colluviosoils, which are incipient soils typically located in depression and valley areas, and are subdivided into non-calcareous, calcareous, and humic non-calcareous, the latter being the most predominant in the region. These soils are the result of a gradual "filling" process through sediments brought by river bodies and by the action of the wind and thereby forming the Aveiro sedimentary basin.

This basin is predominantly composed of alluvial sedimentary materials, including sandstones and clayites. According to Teixeira and Zbyszewski (1976), the main geological units present in Aveiro region (Fig. 1) and within the BVL comprise: Modern Deposits (Quaternary) (current alluvium, beach and dune sands, among others); Cenozoic: Ancient beach deposits, River terrace deposits and Residual blocks; Mesozoic: Cretaceous (Sandstones and clays of Aveiro, Sandstones of Mamodeiro, Limestone and Gray clays of Carrajão and Sandstones of Requeixo); Mesozoic: Late Triassic; Schist-Greywacke Complex before Ordovician Clayey schists (Arada schists). As previously mentioned, this study aims to correlate the satellite data with geological parameters in order to assess their influence on the soil's spectral response.

2.2. Satellite data and research framework

This research differentiates and classifies the different areas of BVL based on satellite imagery from the MSI/Sentinel 2B satellite with spatial resolution of 10m and 20m, temporal resolution of 5 days and radiometric resolution of 12 bits. The satellite data acquired were related to the dates of 13 July of 2023 and 03 February of 2024, in order to be able to identify differences in salinity in the summer and winter season, respectively. The imagery acquired between July 2023 and February 2024 was selected for this study to ensure the use of recent and high-quality data that accurately represent the current environmental conditions of the study area. Although the field samples date from the 2018 sampling campaign, this dataset was retained due to its reliability and spatial representativeness. Given that new field sampling campaigns are logistically demanding and financially costly, the acquisition of updated in situ data was not feasible for the present research context. The images obtained were corrected in their geometry (orthorectified), referenced to the WGS-84 global reference system and projected in the UTM projection system.

The sample geochemical data were applied based on previous research conducted by Melo (2018) with a total of 102 samples collected in the period of May, July, September and October of 2018. A total of 51 sampling points were selected, with samples collected at two depths intervals: 0 to 25cm and 25 to 50cm. The upper layer (0 to 25 cm) was considered the most relevant for the current work as remote sensing primarily reflects the spectral response of the soil surface and vegetation cover. In the laboratory, the samples were first oven-dried at 40 ºC to remove moisture, followed by sieving to obtain fractions smaller than 2 mm. The electrical conductivity values, used as salinity indicator, were determined with a WTW LF 92 conductivity meter on the previously prepared samples. A step-by-step summary of the methodological procedures is illustrated in the flowchart presented in figure 2.

Image pre-processing was conducted using the plugin "Semi-Automatic Classification Plugin" (SCP) integrated within Quantum Geographic Information System (QGIS) software version 3.34.5. Atmospheric correction operations were carried out through the Dark Object Substration (DOS1) method, followed by the conversion of the digital number (DN) into top-of-atmosphere (TOA) reflectance values.

With the aim of mapping saline soils within the BVL region, a preliminary assessment of the vegetation conditions influenced by saline intrusion was performed through bibliographical review and field survey in order to identify the most suitable spectral indices for the study area.

Subsequently, spectral indices were computed using multispectral imagery from the Sentinel 2B sensor system. The selected indices exhibited a stronger reported correlation with geochemical salinity parameters specifically electrical conductivity and pH, as evidenced in previous scientific research such as Kurbatova *et al.* (2021), Boucchima *et al.* (2018) and Barreto (2019). The vegetation indices (Tab. 1) and salinity indices (Tab. 2) were integrated to account for the presence, of undergrowth and shrubs in the BVL area, which complexifies the identification and mapping of soil salinity.

The main vegetation index used was the Normalized Difference Vegetation Index (NDVI), primarily applied to assess vegetation cover, its condition, and to distinguish it from water bodies, bare soils, and urban areas. The Soil Adjusted Vegetation Index (SAVI) is similar to NDVI and varies according to the amount of green vegetation cover. The Canopy Response Salinity Index (CRSI) was idealized to assess vegetation vigor and, therefore, determine the soil salinity. The Normalized Difference Water Index (NDWI) and Normalized Difference Moisture Index (NDMI) represent water content in surface bodies and vegetation cover, respectively. The NDMI highlights differences in leaf water content, allowing the identification of water stress in crops, while the NDWI reflects variations in water content in surface water using the GREEN and NIR bands. For both indices, value above zero indicates healthy vegetation without water stress and well-defined water bodies (Santos *et al*. 2021). Salinity Indices (SI) are used to detect the spectral response of salt minerals on the soil surface (Elhag and Bahrawi, 2016). The main salinity indices applied in this study were the Normalized Difference Salinity Index (NDSI) and Sentinel-2-Based Vegetation Salinity Index (SVSI), both designed to evaluate soil salinity while also characterizing the vegetation vigor. The remaining salinity indices were developed to assess the relationship between spectral bands and surface features, being fundamental for mapping soil salinity.

The indices, shown above, were subsequently correlated with the geochemical salinity parameters for the BVL, obtained as part of the research carried out by Melo (2018). The correlations were performed using electrical conductivity data through the Statistical Package for Social Sciences (SPSS*)* software, version 28.0.1.0 (142) applying Pearson's correlation method. The Pearson correlation coefficient (R) ranges from -1 to +1, where values close to -1 indicate an

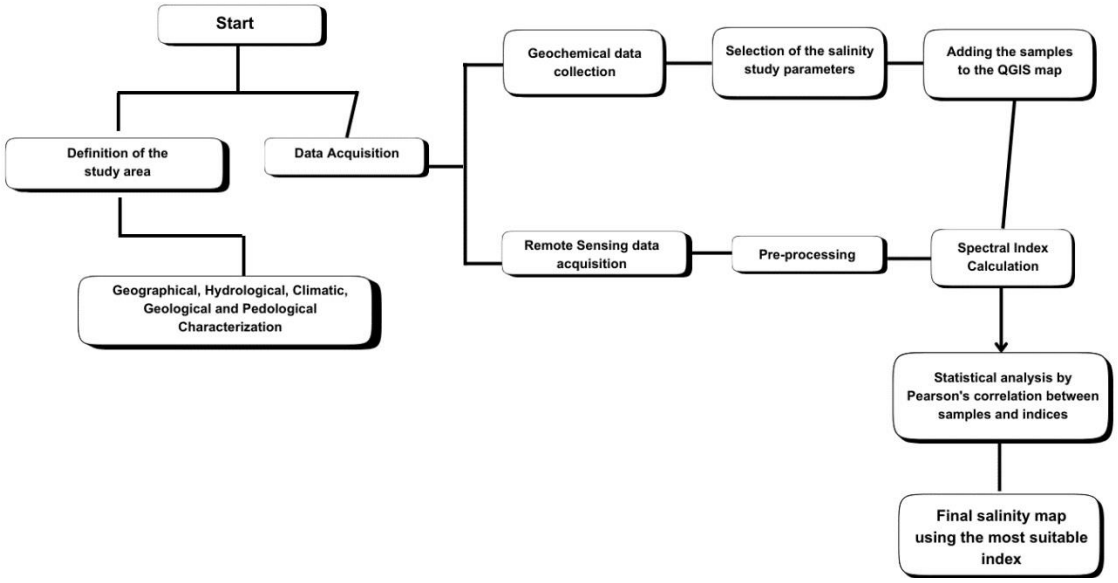

Figure 2. Flowchart of the methodology used to conduct the work.

Figura 2. Fluxograma da metodologia utilizada no desenvolvimento do trabalho.

inverse relationship, and values near 0 indicates the absence of similar variation (Campos and Licht, 2020). The resulting correlation coefficients were classified according to Cohen's criteria (as cited in Suhaili *et al.*, 2019) as weak, moderate or strong (Tab. 3), thereby enabling the selection of the indices that are more representative of the current soil salinity in the study area. More complex statistical analysis was not applied, as the purpose of this study was to achieve consistent and interpretable results using simple and effective statistical tools.

A land use classification was performed using a comparative approach, based on the results of the calculated indices, specifically NDVI, SAVI, and NDWI, in order to evaluate vegetation cover within the processed images. The classification culminated in the following categories: a) type of vegetation; b) exposed soil; c) bodies of water; d) urban areas. The resulting analysis was consistent with the characteristics of halophytic vegetation reported in Almagro *et al.* (2006) and a salinity map was attained based on the index exhibiting the strongest correlation with geochemical parameters.

Table 1. Vegetation and water spectral indexes. Legend: NIR- Near Infrared Band, RED- Red Band, G- Green Band, SWIR1- Shortwave Infrared Band, B- Blue Band.

Tabela 1: Índices espectrais da vegetação e da água. Legenda: NIR - Banda do infravermelho próximo, RED - Banda vermelha, G - Banda verde, SWIR1 - Banda do infravermelho de onda curta, B - Banda azul.

Spectral Indices	Mathematical Formula	References
Normalized Difference Vegetation Index	$NDVI = \frac{NIR-RED}{NIR+RED}$	(Rouse *et al.*, 1974)
Soil Adjusted Vegetation Index	$SAVI = \frac{(NIR - RED)}{(NIR + RED + L)} * (1 + L)$	(Huete, 1988)
Canopy Response Salinity Index	$CRSI = \sqrt{\frac{(NIR * RED) - (G * B)}{(NIR * RED) + (G * B)}}$	(Scudiero *et al.*, 2016)
Normalized Difference Moisture Index	$NDMI = \frac{(NIR-SWIR1)}{(NIR+SWIR1)}$	(Gao, 1996)
Normalized Difference Water Index	$NDWI = \frac{(G-NIR)}{(G+NIR)}$	(McFeeters, 1996)

Table 2: Salinity Indices used in the salinity mapping of the BVL.

Tabela 2. Índices de salinidade utilizados no mapeamento da salinidade do BVL.

Spectral Indices	Mathematical Formula	References
Normalized Difference Salinity Index	$\mathrm{NDSI} = \frac{RED - NIR}{RED + NIR}$	(Khan *et al.*, 2001)
Sentinel-2-Based Vegetation Salinity Index	$\mathrm{SVSI} = \frac{RED - B}{RED_{EDGE1(B5)} + SWIR1}$	(Lugassi *et al.*, 2017)
Salinity Index 1	$\mathrm{SI}\ 1 = \frac{G}{RED * NIR}$	(Abbas and Khan, 2007)
Salinity Index 2	$\mathrm{SI}\ 2 = \sqrt{B * RED}$	(Khan *et al.*, 2001)
Salinity Index 3	$\mathrm{SI}\ 3 = \sqrt{G^2 + RED^2}$	(Douaoui *et al.*, 2006)
Salinity Index 6	$\mathrm{SI}\ 6 = \frac{B - RED}{G}$	(Abbas and Khan, 2007)
Salinity Index 7	$\mathrm{SI}\ 7 = \sqrt{RED^2 + NIR^2}$	(Scudiero *et al.*, 2016)
Salinity Index 8	$SI\ 8 = \sqrt{G * RED}$	(Khan *et al.*, 2005)
Salinity Index 9	$\mathrm{SI}\ 9 = \sqrt{G^2 + RED^2 + NIR^2}$	(Khan *et al.*, 2005)
Salinity Index 10	$\mathrm{SI}\ 10 = \frac{RED}{NIR}$	(Douaoui *et al.*, 2006)

3. Discussion of Results

Initially, the NDVI, SAVI and NDWI indices were calculated, so that the existing differences in land use were amplified. The main classification was based on NDVI values, supported by visual interpretation in Google Earth, allowing an accurate identification

Table 3 Classification of correlation coefficient (R) values according to their magnitude (adapt.ed from Suhaili et al., 2019, based on Cohen, 1988).

Tabela 3. Classificação dos valores do coeficiente de correlação (R) de acordo com a sua magnitude (adaptado de Suhaili *et al*., 2019, com base em Cohen, 1988).

R value (-1.00>R>+1.00)	Relationship Interpretation
0.10 - 0.29	Weak
0.30 - 0.49	Moderate
0.50 - 1.0	Strong

of the best fitting classes for the study area. The NDVI for February presented a minimum value of -0.7334984 and a maximum of 0.9954898, whereas for July the minimum was -0.9980564 and the maximum 0.7367753. This reduction in maximum values indicates a decrease in healthy vegetation cover during summer, likely associated with high temperatures and low precipitation rates that increases water stress and so affects plant growth.

In July 2023, as can be seen in figure 3a, 4 classes were defined: the blue class represents bodies of water; the yellow class, exposed soil or undergrowth; the light green class, medium vegetation; and the dark green class, healthier and denser vegetation. The month of February 2024 (Fig. 3b) presented another class, represented by a light blue color and which detects areas close to bodies of water or urban areas. It is important to note that the classification ranges defined for the summer and winter images were not equivalent, as the minimum and maximum index values varied significantly between seasons in all indices calculated. This variation reflects natural changes in soil moisture, vegetation cover, and atmospheric conditions that influence the spectral response of the surface, as discussed in Santos *et al.* (2024). Therefore, the use of distinct class intervals was necessary to ensure that the classification remained representative of each period, even though it limits direct comparison between the two datasets.

Through the analysis of figure 3, a significant increase in the class corresponding to exposed soil or undergrowth can be observed, as well as a decrease in water body areas during July, resulting from the reduced rainfall in the region. Despite this, in the "Bocage" area, and in the southeastern sector adjacent to the tidal protection dike, an increase in healthy and dense vegetation is evident, which may correspond to the vegetation growth peak and irrigation maintenance associated with agricultural activity in the area. The predominance of undergrowth near the tidal protection dike, observed both in the warmer and wetter seasons, is in accordance with the assumptions of Weier and Herring (2000), who state that vegetation of this size exhibits NDVI values from 0.2 to 0.3, enabling an initial estimation of the halophyte cover, as these species are commonly associated with undergrowth to shrub formations.

The calculation of the SAVI and NDWI indices, similarly to the NDVI, allowed the detection of areas characterized by lower vegetation vigor and greater water stress, as being the closest to the area of saline invasion. Visually, the images generated from the July 2023 dataset revealed a clearer delimitation of the vegetation areas s that are presented as healthy and stressed, whereas in February 2024 these boundaries were not well defined.

This interpretation has a direct influence on the way indices correlate across different times of the year, since plants resist higher salinity values under cold and humid climates than in hot and dry conditions (Maas, as cited in National Research Council, 1990). This will imply changes at the physiological level of the plants, thus allowing a better identification of the halophytes. The increase in salinity means that plants need more energy for the biochemical adjustment necessary to adapt to the new salinity conditions (Holanda *et al*. 2016)), and the warm season therefore appears to provide the most promising results for remote sensing analysis in these environments.

Table 4a shows a moderate positive correlation for the NDSI (0.377) and SI 10 (0.378) indices and a moderate negative correlation for the NDVI (-0.377), SAVI (-0.420), CRSI (-0.428) and SI 2 (-0.426) indices. The stronger positive correlations were obtained in the SI 1 (0.516) indices and the negative correlations for the SI 7 (-0.501) and SI 9 (-0.503) indexes, highlighted in green. Therefore, the salinity index that best portrayed the salinity status of the Baixo Vouga Lagunar was SI 1. In contrast to the findings of Ren *et al*. (2018), the SAVI index showed a moderate correlation in both seasons analyzed, indicating its potential applicability for identifying halophytic vegetation in environments with moderate to low salinity levels.

Regarding the correlations for the month of February, presented in table 4b, there is a notable decrease in the value obtained compared to those from July. This result aligns with the assumption of Maas and Hoffman (as cited in Dias *et al.*, 2016), supporting the interpretation that the hot and dry season produces the most suitable conditions for assessing soil salinity in the BVL region. During the wet and cold season, there is greater water potential and greater drainage of the salts formed, promoting a better vegetation development, since the presence of salts

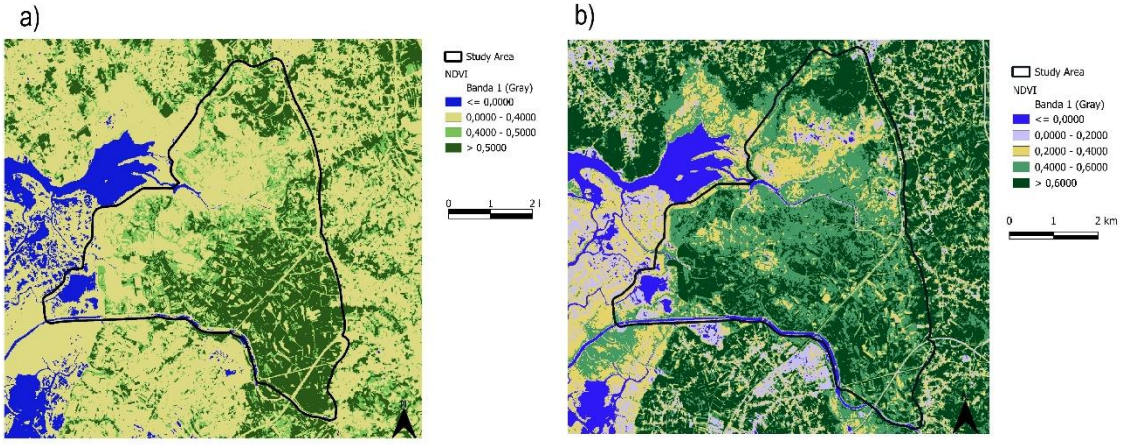

Figure 3. a) NDVI for the month of July 2023, b) NDVI for the month of February 2024.

Figura 3. a) NDVI para o mês de julho de 2023, b) NDVI para o mês de fevereiro de 2024.

Table 4. a) Values of correlations for July 2024, b) values of correlations for February 2023.

Tabela 4. a) Valores das correlações para julho de 2024, b) valores das correlações para fevereiro de 2023.

Spectral Indices	a) Sample Correlation for July 2024	b) Sample Correlation for February 2023
NDVI	-0.377	-0.226
SAVI	-0.420	-0.307
NDMI	-0.242	-0.120
NDWI	-0.124	0.094
CRSI	-0.428	0.270
NDSI	0.377	0.226
SI 1	0.516	-0.263
SI 2	-0.426	-0.061
SI 3	0.026	-0.175
SI 6	0.010	-0.176
SI 7	-0.501	-0.331
SI 8	0.217	-0.246
SI 9	-0.503	-0.338
SI 10	0.378	0.090
SVSI	0.130	0.232

negatively affects plant metabolism and growth, as described by Gaikwad *et al*. (2024).

The vegetation index that obtained the highest correlation was the Vegetation Cover Response Salinity Index (CRSI), where from figure 4 it is possible to verify, in relation to the month of July, a delimitation of zones where halophyte vegetation is predominant and, therefore, with higher salinity values. The decreases in the correlations in the two analyzed epochs can be visualized by comparing the salinity indices SI 7 and SI 9 (Fig. 5).

The indices that exhibited the stronger correlation values were those incorporating the spectral bands: B8 (NIR), B3 (GREEN) and B4 (RED). These findings are in agreement with Metternicht and Zinck (1997), who reported that saline soils with surface salt crystals display high reflectance in the NIR and RED bands whereas darkened saline soils exhibit a decrease in reflectance. Consequently, the lowest spectral values corresponding to the saline zones of the BVL are characterized by reduced reflectance, which translates into moderate to strong correlations with the spectral indices.

In the indices generated for July 2023, there is a predominance of higher salinity classes near the protection dike, where it was previously identified as the area with the highest proportion of plants adapted to salinity. In contrast, in February 2024, the higher salinity classes, represented in pink, appear more spatially dispersed due to increased water circulation and drainage (Fig. 5b, d).

Accordingly, the final salinity mapping of the BVL was based on the SI 1 index (Fig. 6), which presented a correlation value of 0.516 during the warm season, considered the most suitable period for detecting halophytic vegetation.

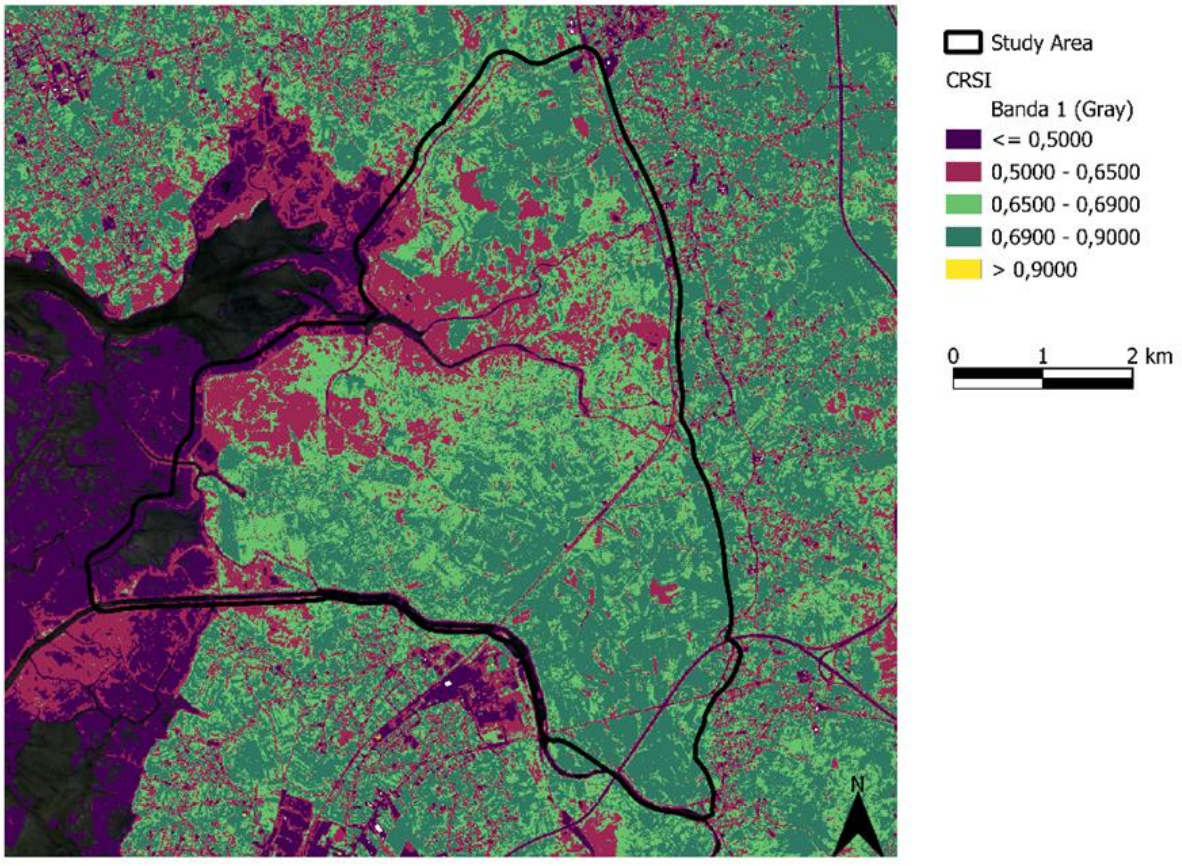

Figure 4. CRSI index for the month of July 2023 with visible delimitation of the areas most affected by salinity in pink.

Figura 4. Índice CRSI para o mês de julho de 2023 com delimitação visível dasmais afetadas pela salinidade em rosa.

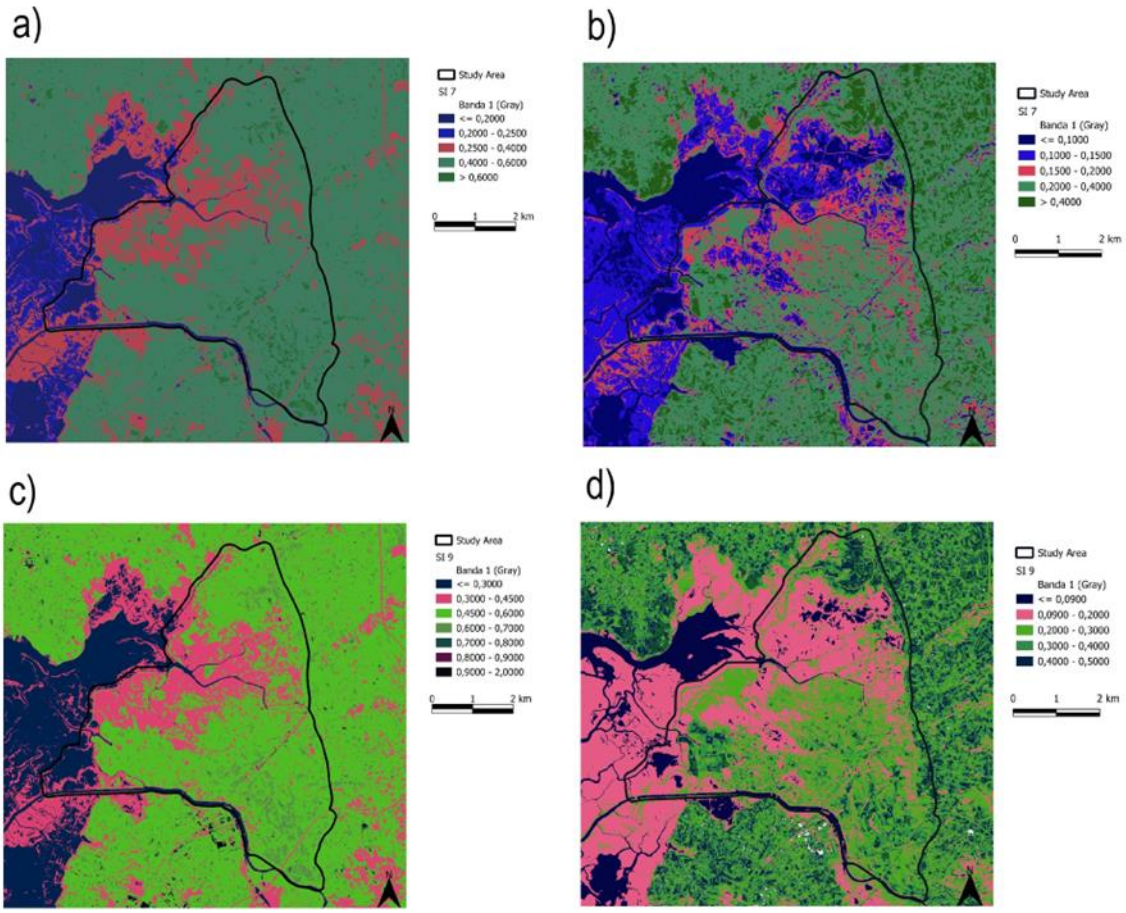

Figure 5. a) SI 7 index for the month of July 2023, b) SI 7 index for the month of February 2024, c) SI 9 index for the month of July 2023, d) SI 9 index for the month of February 2024.

Figura 5. a) Índice SI 7 para o mês de julho de 2023; b) índice SI 7 para o mês de fevereiro de 2024; c) índice SI 9 para o mês de julho de 2023; d) índice SI 9 para o mês de fevereiro de 2024.

The lower classes, represented in dark green and light green tones, correspond to areas of healthy vegetation or undergrowth, as well as certain urban centers. The pink class denotes the onset of salinization, while the subsequent classes represent zones of permanent waterlogging or water bodies. The pink class is particularly evident along the area of the protection dike, delineating the zone of highest salinity within the Baixo Vouga Lagunar (BVL), which is predominantly composed of halophytic and sub-halophytic plants.

It is then possible to characterize, through remote sensing, the salinity of the BVL as a gradual system. In the saline water intrusion zone, higher salinity levels are confirmed by Electrical Conductivity analysis of samples and by the reflectance patterns emitted by the halophytic vegetation in the same area. This zone transitions into an area of lower salinity, where the development of glycophytic plants, i.e., not adapted to salinity and with a significant increase in reflectance becomes more evident, accompanied by an increase in reflectance characteristic of healthy vegetation. This behavior translates into a decrease in spectral values in the SI1 index, indicating absence or reduction of salinity.

Finally, the dark green areas correspond to non-saline soils suitable for agriculture use. These areas are the focus of protective measures aimed at mitigating the advance of salinity, in order to maintain the characteristic landscape of cultivated fields and pastures, which are essential to the economic and sustainable development of the region.

The alluvial soils of the BVL are dark in color due to the high content of organic matter and their tendency to remain periodically soaked, a factor that is explained by the geology of the area, which is predominantly clayey and sandy with low permeability. This factor has favored the accumulation of salt during periods of saline intrusion, subsequently leading to agricultural abandonment, and the proliferation of plant species adapted to such conditions.

4. Conclusion

The mapping of the salinity of the Baixo Vouga Lagunar (BVL) is a challenging process due to the dynamism that the system presents as a wetland. One of the main limitations is the presence of halophytic vegetation and the reduced permanence of exposed soils. Even so, the vegetation and salinity indices exhibited consistent results to support the analysis. It was observed that July represents the most suitable period for detecting saline indicators, as the surrounding areas show greater spatial definition and more pronounced spectral characteristics. Conversely, the wetter month of February exhibited lower correlations and a combination of conditions that did not identify the study parameters.

The index that best represented the study area was SI1, which achieved a correlation of 0.516 in July and was therefore selected

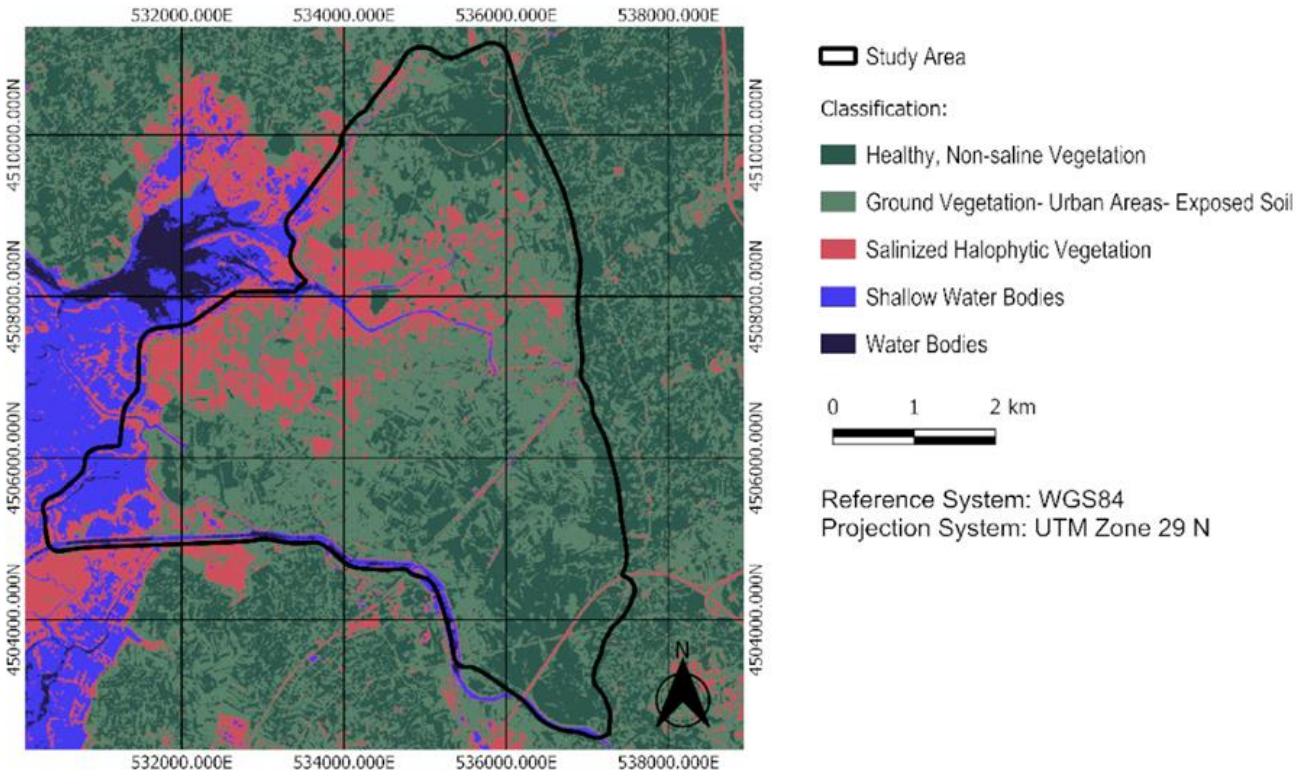

Figure 6. BVL Salinity Map for the month of July 2023 and representative of the current state of soil salinity.

Figura 6. Mapa de salinidade para o mês de julho de 2023, representativo do atual estado de salinidade do solo.

for the salinity mapping of the BVL. Other salinity indices, such as SI7 and SI9, showed promising results, with strong correlations in July and moderate ones in February. Among the vegetation indices, the SAVI stood out for presenting a moderate correlation in both periods, and, together with other indices such as the CRSI, can be considered a reliable indicator of halophytic vegetation, thus enabling the delimitation of soils affected by salinity.

The geological features of the soil indicate that the darkest soils are generally more saline and display lower spectral responses compared to lighter soils. These darker soils are periodically saturated due to the variation in sea water levels and their low permeability. Its low permeability is attributed to the high content of clay and fine silty organic materials, which limit salt leaching and favor its prolonged retention in the soil. This relationship highlighted the importance of correlating geological data with satellite-derived information.

The model applied in this study can be replicated in other wetlands across the country, which also suffer from the problem of saline intrusion, serving as a reference for targeted research or monitoring of salinity dynamics. The accuracy of results obtained can be further improved through the use of higher spatial resolution imagery, such as that obtained from hyperspectral sensors, which would enable the generation of more detailed maps capable of representing the different intensities of salinity within the study area.

This research holds significant local relevance, as it characterizes processes that directly affect the population dependent on this region for their livelihood. Furthermore, it was also a point of immense interest to understand halophytic behavior in contrast with glycophytes and their respective spectral responses, thereby encouraging more detailed investigations in future studies.

Acknowledgements

This work was supported by GeoBioTec - Geo (UIDB/04035) Research Centre, funded by National Funds through FCT. The authors declare that the research was conducted in the absence of any commercial or financial relationships that could be construed as a potential conflict of interest.

References

Abbas, A., Khan, S., 2007. Using Remote Sensing Techniques for Appraisal Irrigated Soil Salinity. *In*: MODSIM07 - *Land, Water and Environmental Management: Integrated Systems for Sustainability.*

Almagro, M., Marín, G., Lopes, R., Pinho, C., Keizer, J., 2006. Monitorización de la flora y vegetación de las zonas húmedas en el Baixo Vouga Lagunar (Ría de Aveiro). *Ecosistemas*, **15**: 72-82.

Barreto, A., 2019. *Modeling Soil Salinity Using Remote Sensing Techniques*. [Doctoral Dissertation]. Federal Rural University of the Semi-Arid Region; https://doi.org/10.21708/bdtd.ppgmsa.tese.5180.

Bouchhima, R. A., Sarti, M., Ciolfi, M., Lauteri, M., Ksibi, M., 2018. Decision tree for mapping of halophyte cover around Ghannouch, Tunisia. *Environ Monit Assess,* **190**:742. https://doi.org/10.1007/s10661-018-7115-3.

Bratovcic, A., 2024. Different approaches to reduce salinity in salt-affected soils and enhancing salt stress tolerance in plants. *Agricultural Science*; **15**: 830-847. https://doi.org/10.4236/as.2024.158046.

Cardoso, J. V. J. C., 1974. A Classificação dos Solos de Portugal - Nova Versão. *Boletim Solos (SROA),* **17**: 14-46.

Campos, F. F., Licht, O. A. B., 2021. Correlation diagrams: Graphical visualization of geochemical associations using the EzCorrGraph app. *Journal of Geochemical Exploration*, **220**: 106657. https://doi.org/10.1016/j.gexplo.2020.106657.

Dias, N., Blanco, F. F., Souza, E. R., Jorge, F. F., Neto, O. N., Queiroz, I. S. R., 2016. Effects of salt on the plant and tolerance of crops to salinity.

In: Gheyi, H., Dias, N., Lacerda, C., Gomes, F. (Eds.), *Salinity management in agriculture: basic and applied studies*, Institute Nacional de Ciencia e Tecnologia em Salinidade, 151-162.

Douaoui, A., Nicolas, H., Walter, C., 2006. Detecting salinity hazards within a semiarid context by means of combining soil and remote-sensing data. *Geoderma,* **134**: 217-230. http://dx.doi.org/10.1016/j.geoderma.2005.10.009.

Elhag, M., Bahrawi, J. A., 2016. Soil Salinity Mapping and Hydrological Drought Indices Assessment in Arid Environments Based on Remote Sensing Techniques. *Geoscientific Instrumentation Methods and Data Systems*, **6**: 39. https://doi.org/10.5194/gi-2016-39.

Gaikwad, A. S., Bhakare, B. D., Kamble, B. M., Thakare, R. S., Durgude, A. G., 2024. Soil microbiome: Applications and mechanisms for salinity stress mitigation in plant and soil ecology – A review. *Biochem. J.*, **8(3)**: 875. https://doi.org/10.33545/26174693.2024.v8.i3k.87.

Gao, B., 1996. NDWI—A normalized difference water index for remote sensing of vegetation liquid water from space. *Remote Sens of Environ.*; **58(3)**: 257-266. https://doi.org/10.1016/S0034-4257(96)00067-3.

Holanda, J. S., Amorim, J. R., Neto, M. F., Holanda, A. C. S., Sá, F. V., 2016. Water Quality for Irrigation. *In*: Gheyi, H., Dias, N., Lacerda, C., Gomes, F., editors. *Salinity management in agriculture: basic and applied studies*, Institute Nacional de Ciencia e Tecnologia em Salinidade, 35-50.

Huete, A. R., 1988. A Soil-Adjusted Vegetation Index (SAVI). *Remote Sens Environ,* **25**: 295-309. https://doi.org/10.1016/0034-4257(88)90106-X.

Khan, N., Rastoskuev, V. V., Sato, Y., Shiozawa, S., 2005. Assessment of hydrosaline land degradation by using a simple approach of remote sensing indicators. *Agric Water Manag,* **77**: 96-109. http://dx.doi.org/10.1016/j.agwat.2004.09.038.

Khan, N., Rastoskuev, V. V., Shalina, E. V., Sato, Y., 2001. Mapping Salt-affected Soils Using Remote Sensing Indicators: A Simple Approach with the Use of GIS IDRISI [Conference Paper]. *In* Asian Conference on Remote Sensing, Nov 5-9, Singapore. https://a-a-r-s.org/proceeding/ACRS2001/Papers/AGS-05.pdf.

Kurbatova, A., Bouchhima, R. A., Grigorets, E. A., Tsymbarovich, P. R., Ksibi, M., 2021. Methodology for mapping soil salinity and halophyte cover using remote sensing data in Kerkennah, Tunisia. *Euro-Mediterr J Environ Integr,* **6**:51. https://doi.org/10.1007/S41207-021-00257-4.

Lopes, R., Andresen, M., 2009. Wetlands – an articulation between agriculture and nature conservation: contributions to a management plan in the Baixo Vouga Lagunar. *In*: Brito, B. R., Alarcão, N., Marques, J., Editors. *Community Development: from Theories to Practices - Tourism, Environment and Educational Practices in São Tomé and Príncipe.* Gerpress, 184-191.

Lugassi, R., Goldshleger, N., Chudnovsky, A., 2017. Studying Vegetation Salinity: From the Field View to a Satellite-Based Perspective. *Remote Sensing*, Feb 1, **9(2)**: 122. https://doi.org/10.3390/rs9020122.

McFeeters, S. K., 1996. The use of the Normalized Difference Water Index (NDWI) in the delineation of open water features. *Int J Remote Sens.*, **17**(7): 1425-1432. http://dx.doi.org/10.1080/01431169608948714.

Melo, M., 2018. *Avaliação do grau de salinização de solos agrícolas do BVL: estado atual e suas consequências* [Master's Thesis]. University of Aveiro. http://hdl.handle.net/10773/25836.

Metternicht, G., Zinck, J. A., 1997. Spatial discrimination of salt- and sodium-affected soil surfaces. *Int J Remote Sens*, **18**(12): 2571-2586. https://doi.org/10.1080/014311697217486.

National Research Council, 1990. Saline Agriculture: Salt-Tolerant Plants for Developing Countries. *Washington, DC: The National Academies Press*. https://doi.org/10.17226/1489.

Ren, H., Zhou, G., Zhang, F., 2018. Using negative soil adjustment factor in soil-adjusted vegetation index (SAVI) for aboveground living biomass estimation in arid grasslands. *Remote Sens. Environ.*; **209**: 439–445. https://doi.org/10.1016/j.rse.2018.02.068.

Santos, F. L. M., Rodrigues, G., Potes, M., Couto, F. T., Costa, M. J., Dias, S., Monteiro, M. J., Ribeiro, N. d. A., Salgado, R., 2024. Moisture content vegetation seasonal variability based on a multiscale remote sensing approach. *Remote Sens.,* **16**: 4434. https://doi.org/10.3390/rs16234434.

Santos, R. de O., Delgado, R. C., Vilanova, R. S., Santana, R. O., Andrade, C. F., Teodoro, P. E., Silva Junior, C. A., Capristo-Silva, G. F., Lima, M., 2021. NMDI application for monitoring different vegetation covers in the Atlantic Forest biome, Brazil. *Weather and Climate Extremes*, **33**: 100329. https://doi.org/10.1016/j.wace.2021.100329.

Scudiero, E., Corwin, D. L., Anderson, R. G, Skaggs, T. H., 2016. Moving Forward on Remote Sensing of Soil Salinity at Regional Scale. *Front Environ Sci*., **4**: 65. https://doi.org/10.3389/fenvs.2016.00065.

Silva, M., 2000. *Aspetos morfológicos e ecofisiológicos de algumas halófitas do sapal da Ria de Aveiro* [Doctoral Dissertation], University of Aveiro.

SROA, 1970. *Carta dos Solos de Portugal. I Vol: Classificação e Caracterização Morfológica dos Solos*. Lisboa (Portugal), Ministério da Economia, Secretaria de Estado da Agricultura, Serviço de Reconhecimento e Ordenamento Agrário.

Suhaili, S., Mahat, H., Hashim, M., Saleh, Y., Nayan, N., & Lukmanulhakim, N. N., 2019. Hierarchy of Multicultural Criteria among Public University Students in Malaysia. *International Journal of Academic Research Business and Social Sciences*, **9**(5): 406-419. http://dx.doi.org/10.6007/IJARBSS/v9-i5/5880.

Teixeira, C., Zbyszewski, G., 1976. *Carta Geológica de Portugal 1:50000. Notícia Explicativa da Folha 16-A Aveiro.* Serviços Geológicos de Portugal.

Vengosh, A., 2014. Salinization and Saline Environments. In: Holland H, Turekian K, editors. *Treatise on Geochemistry*. Elsevier Science, 325-378. https://doi.org/10.1016/B978-0-08-095975-7.00909-8.

Weier, J., Herring, D., 2000. *Measuring Vegetation (NDVI & EVI).* NASA Earth Observatory.